

CONFERENCE PRE-PRINT

PERFORMANCE OF LI- AND SN-FILLED CPS TARGETS UNDER TRANSIENT PLASMA LOADS IN QSPA

I.E. GARKUSHA^{1,2}, V.A. MAKHLAI¹, S.S. HERASHCHENKO¹, YU.V. PETROV¹, Y.E. VOLKOVA¹, N.V. KULIK¹, D.V. YELISYEYEV¹, P.B. SHEVCHUK¹, YU. V. SIROMOLOT¹, T.W. MORGAN³

¹-National Science Center „Kharkiv Institute of Physics and Technology“, Kharkiv, Ukraine.

²-V.N. Karazin Kharkiv National University, Kharkiv, Ukraine

³-DIFFER, Dutch Institute for Fundamental Energy Research, Eindhoven, the Netherlands.

Email: garkusha@ipp.kharkov.ua

Abstract

The erosion behavior of selective laser melting (SLM) tungsten (W) Capillary Porous Structure (CPS) targets filled with lithium (Li) was examined under transient plasma loads in the Quasi-Stationary Plasma Accelerator (QSPA). Plasma pulses (0.25 ms, ~ 3 MJ/m²) were applied to two CPS targets, one oriented normally and the other inclined relative to the incident plasma stream. Observations of plasma-surface interactions revealed particle ejection from the exposed target, which depended on the energy density of the incoming plasma stream. Low-energy exposures (< 1.2 MJ/m²) resulted in only minor particle release, whereas higher loads led to significant ejection with velocities up to 33 m/s. Post-mortem analysis of the CPS target under oblique plasma exposure revealed erosion at the leading edge, pointing to this region as a critical factor in target resilience. A comparative analysis of the damage to Li- and Sn-CPS samples exposed to both inclined and normal plasma streams under conditions simulating transients in a fusion reactor was also performed.

1. INTRODUCTION

The divertor in a tokamak reactor will be subjected to extreme heat and particle loads during transient events such as edge-localised modes (ELMs) and disruptions [1]. In addition to tungsten (W), which is currently selected as the baseline material for plasma-facing components (PFCs), alternative divertor designs incorporating liquid metals (LMs) are undergoing comprehensive assessment [1]. Liquid tin (Sn) and lithium (Li) are among the most promising candidates due to their low melting points, high thermal resilience, and ability to form a vapour shield, resulting in a significant decrease in surface heat load during transient plasma events [2-4].

Li offers low Z and favourable shielding behaviour but raises questions of fuel co-handling and operational windows; Sn provides low tritium retention and practical handling yet is more prone to radiative limits at comparable power exhaust. Predictive simulations for COMPASS-U [2] indicate acceptable Li concentrations with negligible core cooling, whereas Sn can approach radiative disruption at moderate power unless cooling and redeposition are optimized, highlighting material-dependent constraints for reactor scenarios. Both Li and Sn have demonstrated shielding behaviour on linear devices [3-5]. In EAST, the first direct experimental evidence of a lithium vapor shielding effect was obtained, showing that enhanced Li radiation reduced the heat flux to the flowing liquid lithium limiter by more than 50% [6]. In ASDEX Upgrade, experiments with a liquid Sn divertor target demonstrated the presence of a self-regulating vapor shielding layer, which effectively reduced the incident heat flux during both L-mode and H-mode plasmas [7]. Previous experiments at the QSPA facility [8] showed that irradiation of Sn-filled capillary porous structures (CPSs) targets at normal (90°) incidence is accompanied by a strong shielding effect. In disruption-simulation experiments [8], the energy density absorbed by the Sn-CPS target was nearly half of that absorbed by W targets.

LM divertors offer several advantages, including reduced mechanical stress in the liquid state and the ability to replenish eroded material through CPS. However, critical issues, such as droplet ejection, material transport, and plasma contamination, require dedicated simulations and experiments aimed at qualifying LM divertor concepts for a future DEMO-class reactor.

To date, CPS implementations, e.g. woven meshes, felts, sintered blocks, and additively manufactured (SLM/3D-printed) W substrates, have been compared across facilities. In OLMAT, Sn-wetted 3D-printed W-CPS demonstrated the most homogeneous thermal response and withstood up to 58 ± 14 MW m⁻² (100 ms) without

particle ejection or substrate damage [9, 10]. This result highlights the importance of compact, well-bonded architectures for capillary replenishment and heat spreading.

A persistent cross-material challenge is droplet ejection under hydrogen exposure. High-speed observations directly captured bubble-collapse-driven droplet emission from liquid metals; systematic testing shows that operating just above the melting point can increase Sn erosion by orders of magnitude, with CPS reducing, although not eliminating, droplet release relative to free-surface layers. Smaller pores mitigate the size and frequency of ejection, yet thresholds depend on gas/radical/ion conditions and temperature [3].

QSPA experiments with 3D-printed W–Sn CPS demonstrated that targets withstood $\sim 3 \text{ MJ m}^{-2}$ ELM-like pulses ($\approx 0.25 \text{ ms}$) for 100 impacts without significant damage to the W substrate [11]. At oblique incidence, relevant for divertor geometry, particle ejection was observed predominantly from the leading edge of the CPS target [12]. This paper presents comparative experimental studies of plasma-surface interactions during QSPA plasma exposures of Li-CPS prototypes at normal and inclined incidence, along with the analysis of the resulting damage to liquid-metal prototypes as a function of the applied energy loads.

2. EXPERIMENTAL SETUP

Experimental simulations of fusion reactor transient conditions, including relevant surface heat load parameters such as energy density, pulse duration, and particle loads, were performed using the quasi-stationary plasma accelerator QSPA Kh-50 [8, 11-16]. The CPS targets filled with Li have been exposed to the plasma streams with an energy density varied in the range from 0.25 MJ/m^2 up to 3 MJ/m^2 . The plasma loads above 1.1 MJ/m^2 typically cause strong melting and evaporation for pure tungsten samples in QSPA [13], while the smallest load applied is clearly below the W melting threshold. Other parameters of the QSPA hydrogen plasma streams were as follows: the ion impact energy of about 0.4 keV, the plasma stream diameter of 18 cm, and a maximum plasma pressure of 0.32 MPa. The plasma pulse shape was approximately triangular with a pulse duration of 0.25 ms.

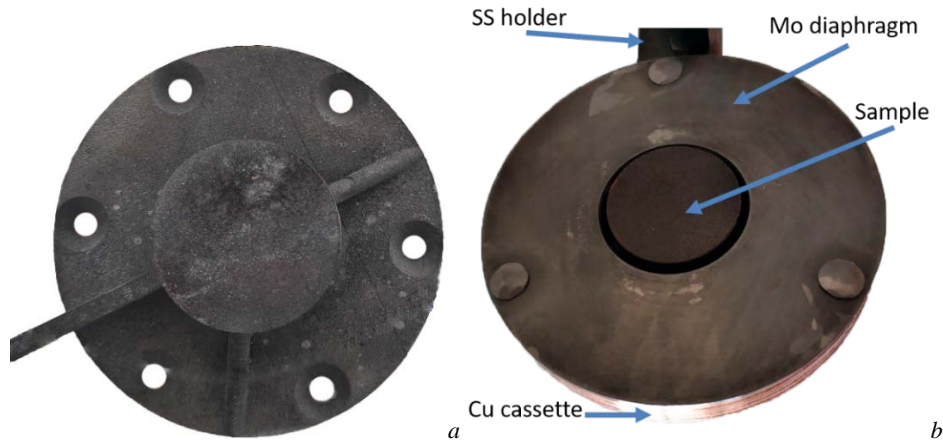


FIG. 1. General view of the CPS target filled with Li in its initial state (a), and the design of the holder used in the experiment (b).

Targets used in the experiments were selective laser melting (SLM) tungsten (W) CPSs filled with Li and provided by DIFFER, with the detailed design described in [17]. The central part of each target, serving as the Li reservoir, had a density of 82%, a diameter of 30 mm, and a thickness of 8.5 mm. Each target contained about 0.5 g of lithium, and the average pore size was $23 \mu\text{m}$. A general view of the CPS sample surface in its initial state is shown in Figure 1 (a). During the experiments, a molybdenum diaphragm was used to protect the holder, as depicted in Figure 1 (b). The initial temperature of the sample (T_{base}) before plasma exposure remained at room temperature ($T_{\text{base}} = \text{RT}$). The surface of one target was oriented normal to the plasma stream (Fig. 2 a), while the other was oriented at an angle of 30° (Fig. 2 b). The main experimental series involved up to 50 plasma pulses. A high-speed digital camera PCO AG (10bit CMOS pco.1200 s) was employed for observing PSI and the ejections of erosion products. The camera had an exposure time ranging from $1 \mu\text{s}$ to 1 s, a spatial resolution of $12 \times 12 \mu\text{m}^2$, and operated within a spectral range from 290 nm to 1100 nm. For clear monitoring of erosion product ejection from the affected surfaces, the exposure of 1.2 ms was selected.

To quantify the overall erosion, mass loss measurements of the targets were performed at regular intervals throughout the experiments. The mass loss after the pulses (ΔM) was determined with an uncertainty of $\pm 15 \mu\text{g}$.

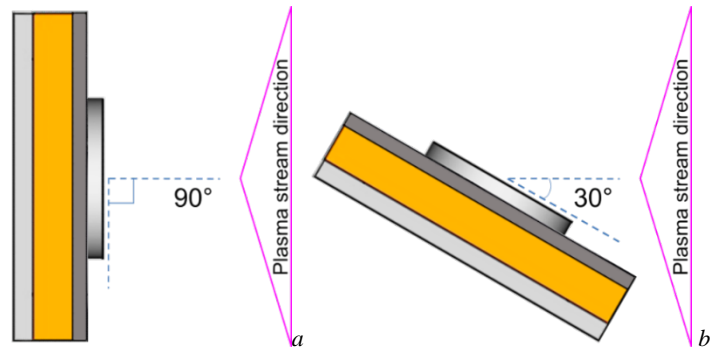


FIG. 2. Schematic view of the plasma exposure in the QSPA facility

3. RESULTS OF EXPERIMENTS

3.1. Plasma-surface interaction

High-speed camera observations of plasma-surface interactions (PSI) during CPS testing under high-intensity QSPA plasma demonstrated particle emission from the exposed targets (Fig. 3-6). The detailed analysis of these observations made it possible to determine the thresholds for particle ejection, which were systematically evaluated under conditions of gradually increasing plasma energy density.

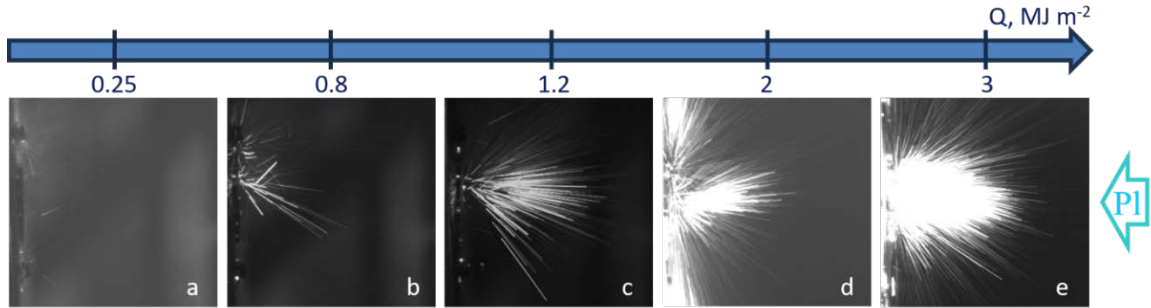


FIG. 3. Energy density of incoming plasma and corresponding images of PSI (a – 0.25 MJ m^{-2} , b – 0.8 MJ m^{-2} , c – 1.2 MJ m^{-2} , d – 2 MJ m^{-2} , e – 3 MJ m^{-2}). The images correspond to 1.2-2.4 ms after the start of the PSI ($t_{\text{exposure}} = 1.2 \text{ ms}$).

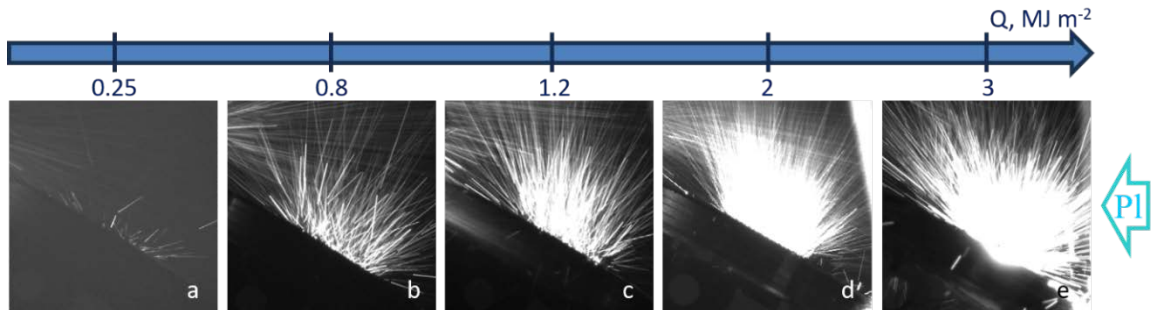


FIG. 4. Energy density of incoming plasma and corresponding images of PSI (a – 0.25 MJ m^{-2} , b – 0.8 MJ m^{-2} , c – 1.2 MJ m^{-2} , d – 2 MJ m^{-2} , e – 3 MJ m^{-2}). The images correspond to 1.2-2.4 ms after the start of the PSI ($t_{\text{exposure}} = 1.2 \text{ ms}$).

In particular, for the CPS target exposed normally to the plasma stream (FIG. 3 a-e), it was found that the first plasma pulses with an energy density below 0.25 MJ/m^2 did not cause any particle ejection from the target surface. Intense particle ejection was recorded in the camera frames at energy densities between 1.2 and 3 MJ/m^2 . The

strongest bursts of droplets were observed at the maximum energy density of the incident plasma flow ($Q = 3 \text{ MJ/m}^2$).

The plasma-surface interaction features in the case of inclined plasma exposure (Fig. 4 a-e) exhibited a similar character to those observed under normal incidence. Particle ejection was also observed, and its intensity strongly depended on the energy density of the incident plasma stream.

For both normal and inclined targets, the particle ejection was observed to occur in a nearly semi-spherical pattern, covering an area close to a 2π solid angle. The velocities of the ejected particles ranged from 1 to 33 m/s, with ejection occurring within the first few milliseconds of exposure. Notably, particles were still observed for more than 7 ms after the onset of PSI (Fig. 5 and 6).

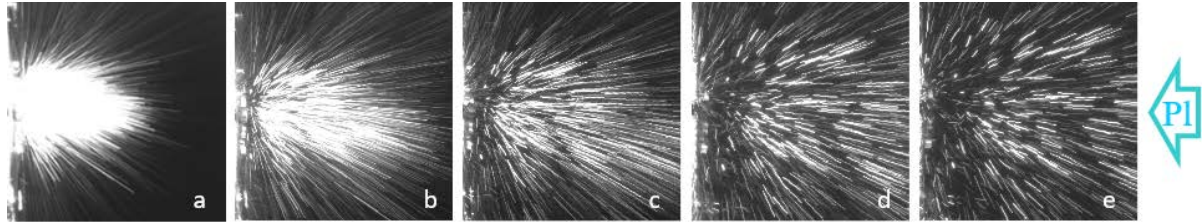


FIG. 5. Images of PSI after a plasma impact on a normally oriented CPS target (with an incoming plasma energy density of 3 MJ m^{-2}). The images correspond to 1.2-2.4 ms (a); 2.4-3.6 ms (b); 3.6-4.8 ms (c); 4.8-6 ms (d); 6-7.2 ms (e) after the start of the PSI ($t_{\text{exposure}}=1.2 \text{ ms}$).



FIG. 6. Images of PSI after a plasma impact on an inclined CPS target (with an incoming plasma energy density of 3 MJ m^{-2}). The images correspond to 1.2-2.4 ms (a); 2.4-3.6 ms (b); 3.6-4.8 ms (c); 4.8-6 ms (d); 6-7.2 ms (e) after the start of the PSI ($t_{\text{exposure}}=1.2 \text{ ms}$).

3.2. Erosion evaluations

Surface analysis of the targets showed that intense QSPA plasma heat loads under normal incidence did not cause any visible changes in the W substrate. In contrast, for the CPS target exposed to inclined transient plasma, damage to the leading edge was observed (Fig. 7).



FIG. 7. General view of the CPS target surface exposed to inclined plasma. Images obtained after 50 plasma pulses.

Particle detachment from the CPS target surface during plasma-surface interactions resulted in a measurable reduction in the target mass. To quantify the effect, the samples were weighed during the experiment. Throughout the entire main experimental series, the normally exposed CPS sample exhibited an average mass loss rate of $0.1 \text{ mg} \cdot \text{cm}^{-2}$ per pulse, while the obliquely exposed target exhibited a higher rate of $0.7 \text{ mg} \cdot \text{cm}^{-2}$ per

pulse. It is important to note that in both cases the total mass loss remained below the initial lithium inventory. Nevertheless, the inclined Li-CPS target experienced greater mass loss than the normally exposed one, most likely due to leading-edge damage.

4. DISCUSSION

The experiments carried out in QSPA Kh-50 have shown that the CPS concept with liquid metal (LM) filling can significantly reduce the energy density of the plasma stream absorbed by the target surface [8]. Moreover, the exposed CPS targets sustained only negligible damage in contrast to the significant damage observed on solid W targets [11, 12]. One of the most critical issues in selecting a liquid metal as the filling material for CPS used as a plasma-facing component is the release of erosion products from the exposed surfaces. It also established that once a certain threshold of plasma energy density was exceeded, particle ejection from the target surface began. The number of ejected particles increased with increasing plasma energy density.

Previous studies have suggested that magnetohydrodynamic (MHD) instabilities at the plasma-liquid interface could be a mechanism for droplet ejection from Sn-filled CPS targets under QSPA irradiation [11]. For Li-filled targets, calorimetric measurements of the absorbed plasma energy relative to the incident energy flux are required to investigate the properties of the vapor shield and to assess particle ejection mechanisms. Such studies are planned for future experiments.

Observations of plasma-surface interactions and erosion analysis demonstrated that for normally irradiated targets, particle ejection occurred uniformly from the entire surface during the main experimental series. At the same time, high-speed camera images showed that particles from inclined targets were predominantly ejected from the leading edge, consistent with the post-exposure appearance of the samples.

The measured mass loss rate for the normally irradiated cold Sn-CPS target was $0.9 \text{ mg}\cdot\text{cm}^{-2}$ per pulse [11] (corresponding to a linear increase in the mass loss coefficient), and $0.128 \text{ mg}\cdot\text{cm}^{-2}$ per pulse for the inclined Sn-CPS [12]. This difference was explained by the formation of a non-uniform shielding layer across the target, which caused an inhomogeneous distribution of the plasma energy on the surface. In particular, only the leading edge of the inclined target absorbed energy densities comparable to those absorbed by the central region of the target under normal incidence [14]. As a result, the average mass loss rate of the normally irradiated Li-CPS was lower than that of the Sn-CPS under equal conditions, which is consistent with the lower atomic mass of Li compared to Sn and with the smaller CPS cell size ($23 \mu\text{m}$ vs $100 \mu\text{m}$, respectively). The opposite trend was obtained for oblique irradiation, where the Li-CPS showed stronger leading-edge damage. The increased mass defect in inclined Li-CPS samples is associated with localized leading-edge damage, where even a small contribution of tungsten substrate erosion is significant, since tungsten is much heavier than lithium. For Sn-filled CPS targets, a similar leading-edge effect was observed [12], although the damage to the tungsten substrate was less pronounced due to the differences in CPS design. This may be related to the differences in the manufacturing technology and structural design of the CPS targets. Future experiments will employ identical CPS designs with different filling metals to enable a more direct comparison.

5. SUMMARY

The erosion of a selective laser melting (SLM) tungsten (W) Capillary Porous Structure (CPS) filled with Li was studied under both normal and oblique high-power plasma exposure in the QSPA. The main experimental series consisted of about 50 QSPA plasma impacts with an energy density of $\sim 3 \text{ MJ/m}^2$ and a pulse duration of 0.25 ms for each target.

The thresholds for particle ejection were analyzed under the conditions of a gradually increasing energy density in the incident plasma stream. The experiment showed that the plasma impacts with energy densities below 1.2 MJ m^{-2} caused only a small number of particles to be ejected from the target surface. At higher plasma loads, the number of ejected particles increased significantly. The velocities of the ejected particles ranged from 1 to 33 m/s. The collection and analysis of erosion products will be addressed in subsequent experiments.

Mass loss measurements indicated that the exposed CPS remained Li-filled during subsequent exposures. Surface analysis of a normally irradiated Li-CPS target did not reveal any visible changes in the W substrate. In contrast, for the Li-CPS target exposed to inclined transient plasma, damage to the leading edge was observed. The damage to the leading edge is a crucial factor contributing to the resilience of the exposed target. Similar effects were

previously observed in experiments with oblique irradiation of castellated W and Sn-CPS targets, where damage occurred due to the formation of a non-uniform shielding layer on the target surface.

Further experiments and detailed studies in QSPA with liquid-metal-filled CPS targets are needed to assess component performance and resilience in fusion reactor conditions.

ACKNOWLEDGEMENTS

This work has been carried out within the framework of the EUROfusion Consortium, funded by the European Union via the Euratom Research and Training Programme (Grant Agreement № 101052200 – EUROfusion). Views and opinions expressed are however those of the author(s) only and do not necessarily reflect those of the European Union or the European Commission. Neither the European Union nor the European Commission can be held responsible for them. Work performed under EUROfusion WP PRD LMD. This work has been supported in part by the Ministry of Education and Science of Ukraine within the project PH/ 56 - 2024. Four members of the team of authors are grateful to the Simons Foundation Program: Presidential Discretionary-Ukraine Support Grants, Award SFI-PD-Ukraine-00014575.

REFERENCES

- [1] You J.H. et al., Divertor of the European DEMO: engineering and technologies for power exhaust, *Fusion Eng. Des.* 175 (2022) 113010.
- [2] Horacek J. et al. Scaling of HeatLMD-simulated impurity outflux from COMPASS-U liquid metal divertor, *Nuclear Fusion* 65 (2025) 016014.
- [3] Scholte J.G. A. et al., Liquid Metal Droplet Ejection Through Bubble Formation Under Hydrogen Plasma and Radical Exposure, *Journal of Fusion Energy* 44 (2025) 22.
- [4] Morgan T.W. et al., Liquid metals as a divertor plasma-facing material explored using the Pilot-PSI and Magnum-PSI linear devices, *Plasma Phys. Control. Fusion* 60 (2018) 014025.
- [5] Rindt P. et al., Performance of liquid-lithium-filled 3D-printed tungsten divertor targets under deuterium loading with ELM-like pulses in Magnum-PSI, *Nuclear Fusion* 61 (2021) 066026.
- [6] Chenglong Li et al., Evidence of vapor shielding effect on heat flux loaded on flowing liquid lithium limiter in EAST, *Plasma Science and Technology* 24 (2022) 095104.
- [7] Scholte J.G.A. et al., Performance of a liquid Sn divertor target during ASDEX upgrade L-mode and H-mode operation, *Nuclear Materials and Energy* 37 (2023) 101522.
- [8] Garkusha I.E. et al., Vapour shielding of liquid-metal CPS-based targets under ELM-like and disruption transient loading, *Nuclear Fusion* 61 (2021) 116040.
- [9] Oyarzabal E. et al., Comparative study of different Sn wetted W CPSs exposed to NBI fluxes in the OLMAT facility, *Fusion Engineering and Design* 190 (2023) 113711.
- [10] Oyarzabal E. et al., Exposure of Sn-Wetted W CPS Targets to Simultaneous NBI Beam and High-Power CW Laser Pulses at the High-Heat Flux OLMAT Facility, *Journal of Fusion Energy* 44 (2025) 3.
- [11] Herashchenko S.S. et al., The CPS's pre-heating effect on the capability to withstand extreme plasma loads, *Fusion Engineering and Design* 190 (2023) 113527.
- [12] Herashchenko S.S. et al., Experimental studies of plasma-surface interactions during inclined QSPA plasma impacts on Sn-filled CPS, *Problems of Atomic Science and Technology* 6(148) (2024) 101.
- [13] Garkusha I.E. et al., Experimental study of plasma energy transfer and material erosion under ELM-like heat loads, *Journal of Nuclear Materials* 390-391 (2009) 814.
- [14] Makhrai V.A. et al., Damaging of inclined/misaligned castellated tungsten surfaces exposed to a large number of repetitive QSPA plasma loads, *Physica Scripta* T171 (2020) 014047.
- [15] Tereshin V.I. et al., Powerful quasi-steady-state plasma accelerator for fusion experiments, *Brazilian Journal of Physics* 32 1 (2002) 165-171.
- [16] Garkusha I.E. et al., Novel test-bed facility for PSI issues in fusion reactor conditions on the base of next generation QSPA plasma accelerator, *Nuclear Fusion* 57 (2017) 116011.
- [17] Morbey M. et al., The role of temperature, deuterium pressure and residual gases in deuterium retention and outgassing of lithium deuterium co-deposits, *Nucl. Fusion* 65 (2025) 106017.